Carbon monoxide hydrogenation over zirconia supported Ni and Co–Ni bimetallic catalysts

Paresh C. Das[1], Naraan C. Pradhan[1,2], Ajay K. Dalai[1]* and Narendra N. Bakshi[1]

[1] *Catalysis and Chemical Reaction Engineering Laboratories, Department of Chemical Engineering, University of askatchewan, Saskatoon SK S7N 5C5, Canada*

[2] *Permanent address: Department of Chemical Engineering, Indian Institute of Technology, Kharagpur, 721 302, India*

Received 22 April 2004; accepted 9 August 2004

Zirconia supported nickel and cobalt–nickel bimetallic catalysts were prepared and characterized for various physico-chemical properties. The hydrogenation of carbon monoxide was studied over these catalysts in the pressure range of 101.3–1654 kPa, temperature range of 513–533 K, weight hourly space velocity range of 8–14 h^{-1} and H2/CO mole ratio of 2. Catalysts containing both Co and Ni were found to give higher C_{5+} hydrocarbons selectivity compared to that containing only Ni. A maximum C_{5+} hydrocarbons selectivity of 55 wt% was obtained at 655 kPa pressure, 523 K and 9.6 h^{-1} of WHSV with catalyst containing 4.03 wt% Co and 2.64 wt% Ni. The C_2 and C_3 olefin contents of the products decreased with increase in pressure. Improved deactivation behavior of the catalysts was observed when operated at high pressure.

KEY WORDS: Fisher–Tropsch synthesis; CO hydrogenation; bimetallic catalyst; nickel; cobalt; zirconia support.

1. Introduction

Petroleum is the major source of gasoline and diesel, the most preferred fuels for the transportation industry. Gradual depletion of petroleum reserves has created interest in finding alternative sources of energy. With the present reserves, natural gas and coal will continue to play a dominating role in the future energy scenario of the world [1]. These materials are very useful for the production of transportation fuels such as gasoline and diesel by Fischer–Tropsch (FT) synthesis.

The increasing importance of FT synthesis can also be realized since the legislative pressure on the maximum level of sulfur and nitrogen emissions from automotive engines is increasing at a faster rate. The diesel and gasoline produced through FT synthesis are of much better quality in terms of sulfur and nitrogen concentrations to meet the future environmental standards. Thus, the FT synthesis perhaps could be the most promising solution for converting non-petroleum based carbonaceous materials to cleaner transportation fuels. However, a major drawback of the process is the low selectivities for gasoline and diesel products. It has been reported that bimetallic catalysts containing Ni, Fe, Co and Ru are more active towards CO conversion, and exhibit markedly improved selectivity for olefins and heavier hydrocarbons as compared to single metal catalysts [2–7]. A large number of combinations of bimetallic catalysts are possible from the above four metals by varying the supports such as silica, alumina, titania, zirconia, zeolites, etc. and preparation procedure. The present work is concerned with the hydrogenation of carbon monoxide over Ni/ZrO_2 and $Co–Ni/ZrO_2$ catalysts.

As mentioned earlier, due to its commercial importance, lot of research works have been and are being done on FT synthesis. It has been reported that the bimetallic catalysts containing Ni, Fe, Co and Ru are more active towards CO conversion and exhibit markedly improved selectivity for olefins and heavier hydrocarbons as compared with single metal catalysts [2–7]. Verma *et al.* [3] studied the performance of MnO supported Co, Ni and Co–Ni bimetallic catalysts at 525–575 K and at atmospheric pressure. Addition of Ni to Co/MnO catalysts produced a stable catalyst with high CO conversion activity. Duvenhage and Coville [4] have studied various physico-chemical characteristics of different $Fe–Co/TiO_2$ bimetallic catalysts. They have identified the formation of Fe–Co alloys on TiO_2 under mild conditions and have not observed any significant difference between TiO_2 supported catalysts and SiO_2 and Al_2O_3 supported catalysts or alloy systems.

Ishihara *et al.* [8] have investigated the hydrogenation of CO over pure Fe, Co, Ni and bimetallic Fe–Co, Co-Ni and Ni–Fe catalysts supported on silica at 523 K and 1.0 MPa. They have reported that, compared to the pure metal catalyst, all the bimetallic catalysts exhibited higher activities for CO conversion and showed enhanced selectivity for heavier hydrocarbons. Amongst all the catalysts studied, 5 wt% Co–5 wt% Ni/SiO_2 was found to be highly active for CO conversion. From

*To whom correspondence should be addressed.
E-mail: dalai@engr.usask.ca

1011-372X/04/1100–0153/0 © 2004 Plenum Publishing Corporation

X-ray diffraction studies, they have concluded that the bimetallic catalysts formed an alloy. From the temperature programmed desorption (TPD) studies, they demonstrated that the alloying of Co and Ni modified the nature of CO and H_2 adsorption resulting in a higher CO conversion and a higher yield of heavier hydrocarbons.

The CO hydrogenation activity of single metal and bimetallic alloy catalysts, selected from Co, Ni and Fe, supported on TiO_2 at a total metal loading of 10 wt% has been studied by Jothimurugesan and Gangwal [9]. The catalysts were prepared by incipient wetness impregnation using nitrate precursor. They reported that alloying of metals resulted in a significant enhancement in CO conversion with low methane selectivity. They also observed that a 50 : 50 weight ratio Co–Ni catalyst physically mixed with HZSM-5 (5% Co–5% Ni/TiO_2 + HZSM-5) gave the highest CO conversion (45.2%, compared to 8.95% and 10.5% with Co-only and Ni-only catalysts, respectively) at the conditions tested. Mixing the Co–Ni catalyst with HZSM-5 resulted in a significant reduction in methane selectivity and a significant increase in C_{4+} selectivity.

Recently, there has been considerable research interest in the use of Ru either alone or in combination with other metals [10–18]. For example, Fan *et al.* [10] have studied the effect of calcination temperature on the performance of supported Ru catalysts for FT reaction. Bruce *et al.* [16] have performed FT synthesis over ruthenium promoted cobalt/ceria coprecipitated catalysts, and reported that the activity of the ceria based cobalt catalyst was enhanced significantly by addition of as little as 0.3 wt% Ru.

Belambe *et al.* [17] have studied the effect of pretreatment on the activity of a Ru-promoted Co/Al_2O_3 FT catalyst. They have observed the pronounced effect of calcination temperature on the overall activity of the catalyst but not on the intrinsic activity of the catalyst sites. On the other hand, the reduction temperature had only a negligible effect on the overall and intrinsic activities. Neither the reduction nor the calcination temperature had any effect on chain propagation. Ruthenium produced large amounts of olefins and heavier hydrocarbons on TiO_2 support [19], whereas, Ni on TiO_2 support improved the selectivity towards heavier hydrocarbons [20]. Bruce *et al.* [21] had studied the CO hydrogenation over $Co–Ni/ZrO_2$ at atmospheric pressure and found the catalyst to be very active and selective for C_{5+} hydrocarbons when compared with its component metals. The C_{5+} hydrocarbon selectivity was more than 60% and the product was rich in 1-ene at the C4–C6 levels.

Fujita *et al.* [22] have reported the use of a series of Ni, Co, Ru, Rh, Pt on different supports for syngas conversion for pyridine methylation applications. They have observed the order of the catalytic acitivity as $Ni/Al_2O_3 > NiZrO_2 > Ni > Ni/SiO_2 > Ni/MgO$ and discussed the relative activities of Ni and Co related to their methanation and methylation activities.

In the present work, a systematic investigation has been conducted to study the effect of Co loading on the physico-chemical characteristics of the $Co–Ni/ZrO_2$ based catalysts and their activity towards CO conversion and selectivity to gasoline range hydrocarbons. The effect of pressure on CO conversion, product selectivity and deactivation behavior of the catalysts has also been studied.

2. Experimental

2.1. Catalyst preparation

Three catalysts having different targeted compositions of Ni and Co were prepared as described below:

(1) 3 wt% Ni on zrO_2–catalyst A
(2) 5 wt% Co and 3 wt% Ni on ZrO_2–catalyst B
(3) 10 wt% Co and 3 wt% Ni on $ZriO_2$–catalyst C.

Catalyst A was prepared by co-precipitation of the mixed solutions of zirconyl nitrate and nickel nitrate by excess alkali solution. 100 g of zirconium dinitrate oxide ($ZrO(NO_3)_2$,H_2O containing 40.1 wt% ZrO_2 supplied by Alpha Products, Danver, USA) and 10 g of $Ni(NO_3)_2 \cdot 6H_2O$ (supplied by BDH Chemicals Ltd., Poole, UK) were each dissolved in 200 mL of distilled water. The two solutions were mixed together and the resulting mixture was added drop by drop with continuous stirring to 400 mL sodium hydroxide (10 wt%) solution. The precipitated mass was filtered and washed repeatedly with distilled water till the filtrate was neutral. After washing with distilled water, the filter cake was washed twice with acetone and then dried in oven at 333 K for 24 h. The catalyst thus prepared was ground sieved to 15–74 μm particle size range.

The other two catalysts (B and C) were prepared by impregnating catalyst A with the required amount of cobalt nitrate solutions. These catalysts were then dried at 333 K for 24 h and ground and sieved to 15–74 μm particle size range.

2.2. Catalyst characterization

The prepared catalysts were characterized using different techniques. The metal contents of the catalysts were determined by atomic absorption (AA) technique.

All the catalysts were pretreated by first calcining them at 773 K for 16 h in air to decompose the impregnated salts. These were then reduced with hydrogen at 725 K for 16 h with a WHSV of 3.6 h^{-1}, prior to the FT synthesis reaction.

Hydrogen and CO chemisorption studies were carried out using a Micromeritics gas absorption apparatus (Model No. 2100D, Instrument Corporation, NJ, USA). Prior to the chemisorption studies, all the

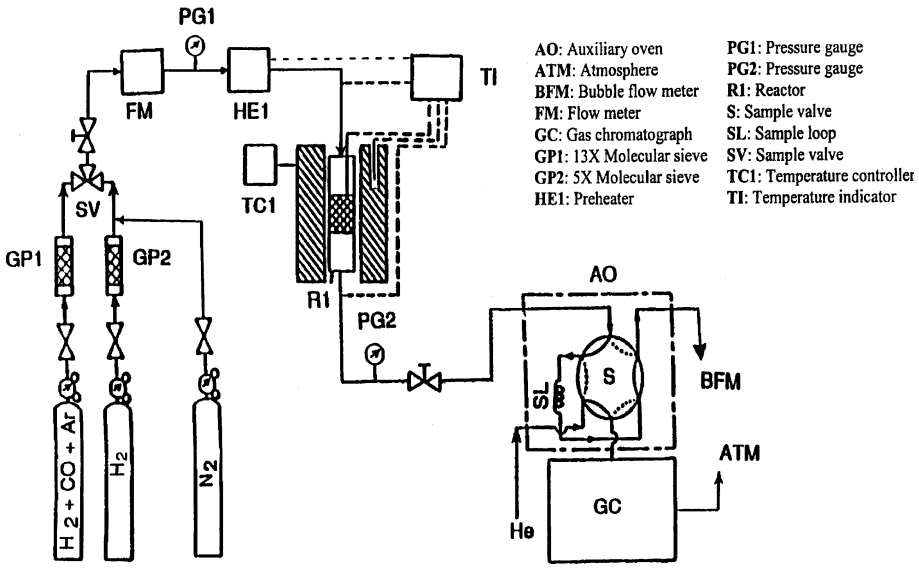

Figure 1. Schematic diagram of the experimental set-up for Fischer–Tropsch synthesis.

catalysts were reduced with hydrogen and then transferred to the adsorption bottle for chemisorption measurement. The samples were again reduced at 573 K *in situ* for 1 h. Following the reduction, the catalysts were degassed for 16 h at 0.2 Pa and 673 K. The catalysts were then cooled to 296 K for the chemisorption measurement. The pressure range for both hydrogen and CO adsorption was 0–33.3 kPa. For both the gases, the total gas uptakes were determined by extrapolating the straight portion of the isotherm to 0.0 Pa pressure.

Temperature programmed reduction (TPR) studies were carried out following the principles outlined by Jenkins *et al.* [23]. The apparatus for the TPR study consisted of a programmable oven, a flow meter, a moisture trap, a thermal conductivity detector (TCD) and a recorder. The feed gas for TPR studies was 3 vol% hydrogen in nitrogen. The catalyst sample was placed inside a quartz tube in the temperature programmable oven. Feed gas at a flow rate of 30 mL/min was passed through one limb of the TCD and entered the quartz tube where it came in contact with the catalyst. Then the feed was vented to the atmosphere through the other limb of the TCD. On the vent line, a bubble flow meter was provided to measure the gas flow rate. In order to remove the moisture formed during reduction, a 5× molecular sieve trap was provided on the gas line. As the catalyst sample placed in the quartz tube was heated at a linear programmed rate the hydrogen consumption due to the reduction of the catalyst was monitored by the TCD and displayed on the recorder. The hydrogen consumption was quantified by means of a calibration with pure CuO, which is known to be reduced completely to Cu. The percentage reduction was calculated from the amount of hydrogen consumed and the amount of total metal oxides present in the catalysts.

X-ray diffraction (XRD) measurements were carried out with a Philips diffractometer (Model no. PW 1310) using CuK^{α} radiation with a glancing angle in the range of 5–85 ° and a scanning speed of 2 °/min.

Scanning electron microscopic (SEM) studies were conducted using a Philips scanning electron microscope operated at 30 kV/SE and 50 ° inclination.

2.3. Experimental set-up

The schematic of the experimental set-up for Fisher–Tropsch synthesis is shown in figure 1. The reactor was a glass-lined stainless steel tube (3 mm I.D.) surrounded by an aluminum block. The whole reactor assembly was kept in an electrical furnace. The temperature of the reactor was controlled to within ±1,°C by means of a temperature controller (TC1). The reactor set-up was also equipped with a multi-point temperature indicator (TI) to measure temperature at various locations.

The product hydrocarbons were analyzed by on-line gas chromatography (Model 5880, Hewlett Packard) through an automatic sampling system. C_1–C_8 hydrocarbons were separated by a Chromosorb 102 column and detected by an FID, whereas the higher hydrocarbons (up to C_{16}) were separated by a SP 2100 column and detected by an FID. The CO and CO_2 contents of the product gas were analyzed by another gas chromatograph (Model 5890, Hewlett Packard) using a Carbosieve SII column and a TCD. The line between GC and FT reactor was maintained at 493 K throughout the experiment to prevent condensation of hydrocarbons present in the product stream.

Table 1
Metal analysis, H_2 and CO chemisorption uptake values for different catalysts

Catalyst	Nickel (wt%)	Cobalt (wt%)	BET surface area (m^2/g)	H_2 chemisorption (μmol/gcat.)	CO chemisorption (μmol/gcat.)	CO/H ratio	Percent reduction
Ni/ZrO_2 (A)	2.83	0.0	88.7	13.0	49.0	1.88	65
$CO–Ni/ZrO_2$ (B)	2.64	4.03	98.8	15.0	31.0	1.03	70
$Co–Ni/ZrO_2$ (C)	2.61	8.06	95.0	28.0	46.0	0.92	77

3. Results and discussion

The metal contents of all the prepared catalysts A–C as determined by AA technique are presented in table 1. The catalysts were also characterized with respect to their physico-chemical properties as well as their activity for CO hydrogenation under various operating conditions. The results obtained from these studies are presented and discussed below.

3.1. Temperature programmed reduction studies

The reduction profiles for all the catalysts are shown in figure 2. It is seen from this figure that the catalyst A shows a maximum reduction temperature of 725 K whereas catalysts B and C show two reduction maxima (640 and 823 K for catalyst B and 640 and 783 K for catalyst C). However, the literature [24] shows that the pure nickel and cobalt oxides under similar operating conditions reduce with a peak maximum of 590 and 640 K, respectively. This indicates that the nickel and cobalt oxides present in catalysts A, B and C reduce at higher temperatures compared to pure nickel and cobalt oxides. This is probably due to the presence of support, which increases the reduction temperatures of nickel and cobalt oxides. Similar observations have been made for other supported catalysts by previous workers [21,25]. It is also observed from the TPR profiles of catalysts B and C that the maximum reduction temperature decreases with increase in cobalt loading. Probably, the increased metal loading reduces the metal–support interaction and the metal oxide reduces with less interference from the support.

3.2. X-ray Diffraction (XRD) studies

The X-ray diffraction patterns of catalysts A and B are shown in figure 3. It is seen from this figure that the peaks for nickel, cobalt and nickel–cobalt alloy are absent, although the peaks for zirconia are observed for both the catalysts. The absence of metal peaks in the XRD spectra indicates that the metal crystallites present in the catalysts are very small in size (<3 nm) and, thus, highly dispersed. In case of catalyst A, high dispersion of metal is also supported by hydrogen and CO chemisorption studies.

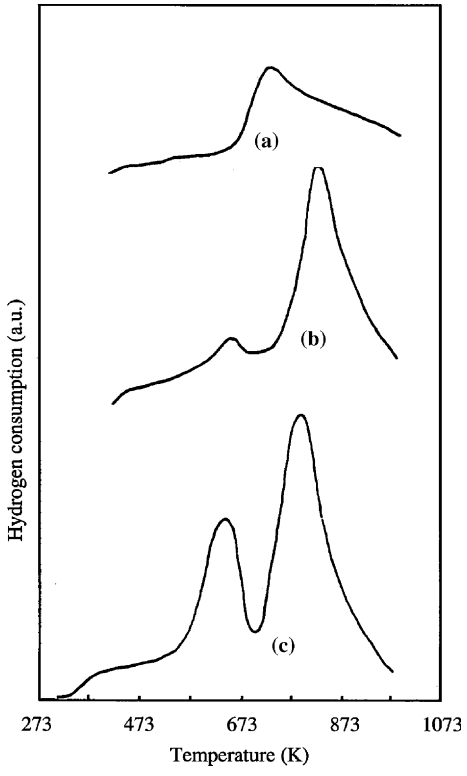

Figure 2. TPR Profiles of Co–Ni bimetallic catalysts a: Ni/ZrO_2 (A); b: $Co-Ni/ZrO_2$ (B); c: $Co–Ni/ZrO_2$ (C).

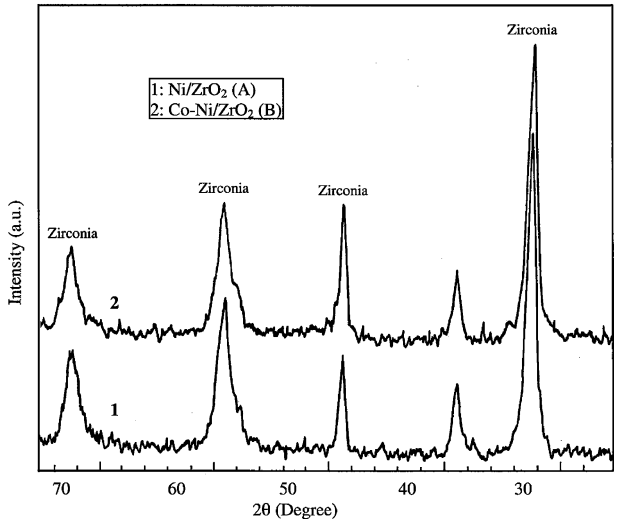

Figure 3. X-ray diffraction patterns of catalysts Ni/ZrO_2 (A) and $Co-Ni/ZrO_2$ (B).

3.3. Chemisorption studies

The metal contents, percent reduction, and hydrogen and carbon monoxide chemisorption uptake values for all the catalysts A– C are presented in table 1. The catalysts possess moderate surface areas ranging from 88 to 99 m^2/g. From the percent reduction values, it is observed that catalyst A has the lowest percent reduction, and the reducibility of the catalysts increases with increase in metal loading. This behavior could be explained on the basis of distribution of metal component in the support matrix. With low metal loading, the metal components are usually highly dispersed throughout the support matrix and are in intimate contact with the support. This increases the extent of support–metal interaction. As a result, some of the oxides could not be reduced. However, with the increase in metal loading, both the dispersion of metal components and the extent of interaction between support and metal decreases.

It is also evident from table 1 that the hydrogen uptake for the catalysts increases with metal loading. As observed from percentage reduction results, the reducibility of the catalysts increases with increase in metal loading. Due to the increase in the extent of reduction with metal loading, more active sites are available for hydrogen chemisorption thus resulting in higher hydrogen uptake values. As can be seen from table 1, the CO uptake values for the catalysts do not follow any regular pattern, which could be due to the complex nature of CO chemisorption.

It is also seen from table 1 that the CO/H absorption ratio for catalyst A is 1.88, whereas for catalysts B and C, this ratio is close to unity. As reported in the literature, in case of supported catalysts, the CO/H ratio indicates the extent of metal dispersion [26]. It is well accepted that the hydrogen is chemisorbed dissociatively such that one atom of hydrogen is absorbed per atom of the active site [26]. Also, the nature of hydrogen chemisorption is independent of metal dispersion. On the other hand, the nature of CO adsorption is markedly affected by the metal dispersion. CO is reported to approach an active site from all directions for a highly dispersed metal situation and 2–3 molecules of CO may be chemisorbed on an active site (carbonyl formation) [26]. Therefore, in the case of highly dispersed metal, the CO/H absorption ratio ranges between 2 and 3. On the other hand, for poorly dispersed metal crystallites, two active sites are shared by one CO molecule (bridge formation) resulting in a CO/H uptake ratio of less than one. However, for moderately dispersed metal crystallites, the ratio is approximately one. It appears, therefore, that the catalyst A, for which the CO/H absorption ratio is 1.88, metal crystallites are present in a highly dispersed form, whereas in catalysts B and C having, CO/H ratios 1.03 and 0.92, respectively, the metal crystallites are present in a moderately dispersed phase.

3.4. Carbon monoxide hydrogenation activity studies

The hydrogenation of carbon monoxide over the series of $Co–Ni/ZrO_2$ catalysts was carried out in the temperature range of 523–633K, WHSV range of 5.6–24.5 h^{-1} and pressure range of 101.3–1654 kPa. The H_2/CO ratio was kept constant at 2 : 1 for all the experiments. The conversions of CO in all experiments were kept at a lower level (<10%) so that the reactor could be considered as a differential one.

3.4.1. Effect of cobalt loading

The effects of Co loading in $Co–Ni/ZrO_2$ catalysts on the conversion of CO and selectivities of different hydrocarbons at a reaction temperature of 533 K, pressure of 101.3 kPa and a WHSV of 12.3 h^{-1} are shown in table 2. It can be seen from this table that the cobalt loading has no effect on the activity of the catalyst for CO hydrogenation as there is almost no change in CO conversion with increase in Cobalt loading. The cobalt loading has, however, strong effect on the selectivity of C_{5+} hydrocarbons as there is a change in C_{5+} selectivity from 21.3 wt% to 39.6 wt% with loading of 4.03 wt% Co to 2.64 wt%Ni/ZrO_2 catalyst (table 2). The C_{5+} hydrocarbon selectivity further improved with increase in Co loading to 8.06 wt%. Table 2 also shows that the $C_2^=$ olefin selectivity increased by 16% upon incorporating 4.03 wt% Co to 2.64 wt% Ni/ZrO_2 catalyst, whereas a nominal change of 3% in $C_3^=$ olefin selectivity was observed with the addition of Co to the Ni/ZrO_2 catalyst. The increased C_{5+} selectivity could be due to suppression of well-known methanation activity of Ni upon addition of Co to it. As $Co–Ni/ZrO_2$ catalysts gave higher C_{5+} selectivity compared to Ni/ZrO_2 catalysts, further experiments were mostly concentrated on bimetallic catalysts.

3.4.2. Deactivation behavior of $Co–Ni/ZrO_2$ catalyst

Figure 4 shows the time-on-stream behavior of catalyst B for CO conversion. Figure 5 shows the variation of C_{5+} hydrocarbon selectivity with time-on stream. It can be seen from these figures that the catalyst is quite stable towards CO conversion activity as well as C_{5+} hydrocarbon selectivity at high pressure (655 kPa). On the other hand, the CO hydrogenation activity and hydrocarbon selectivity steadily fell with time-on-stream. A similar observation was also made for catalyst C. The reason for the improved deactivation behavior of Co–Ni bimetallic catalysts during operation at high pressure could be attributed to the higher hydrogenation activity of these catalysts.

The catalyst deactivation was also observed to be associated with high $C_2^=$ and $C_3^{|dbond}$ olefins selectivity. For example, in the case of operation at atmospheric pressure, there was high selectivity towards $C_2^=$ and $C_3^=$ olefins with faster deactivation of catalysts. On the other

Table 2
Comparison of activities of various catalysts

Catalyst	CO conversion (%)	Selectivity (wt%) of					$C_2^=/\sum C_2$	$C_3^=/\sum C_3$
		C_1	C_2	C_3	C_4	C_{5+}		
Ni/ZrO_2 (A)	4.2	25.1	16.8	22.5	14.3	21.3	0.40	0.86
Co–Ni/ZrO2 (B)	4.6	26.8	7.6	14.6	11.4	39.6	0.56	0.89
Co–Ni/ZrO2 (C)	4.0	22.9	7.7	13.3	10.7	45.4	0.62	0.90

Conditions: temparature, 533 K; pressure, 101.3 kPa; WHSV, 12.3 h^{-1}; H_2/CO ratio, 2.

hand, in case of high pressure run, the product was less olefinic in nature with stable catalytic activity for longer periods. The catalytic activity is, therefore, related to olefin selectivity in some way or other.

It is well established that one of the reasons for the deactivation of FT catalyst is coke formation on the catalyst. Also, olefins are more active and commonly regarded as favored coke precursors as compared to paraffins. Hence, in the present study, formation of more coke precursor olefins at atmospheric pressure leads to faster deactivation of the catalyst. At higher pressure, as the catalysts are more hydrogenating in nature, olefin formation decreases with improved deactivation behavior of the catalyst.

3.4.3. *Effect of pressure*

The effect of pressure on conversion of CO was studied by varying the pressure from atmospheric to 1654 kPa. As shown in figure 6, pressure had very little effect on CO conversion over catalyst A, whereas it had strong effect on CO conversion activities of catalysts B and C upto a pressure of 655 kPa and then leveled off. The increase in CO conversion with increase in pressure is due to improved activity of the catalysts at higher pressures.

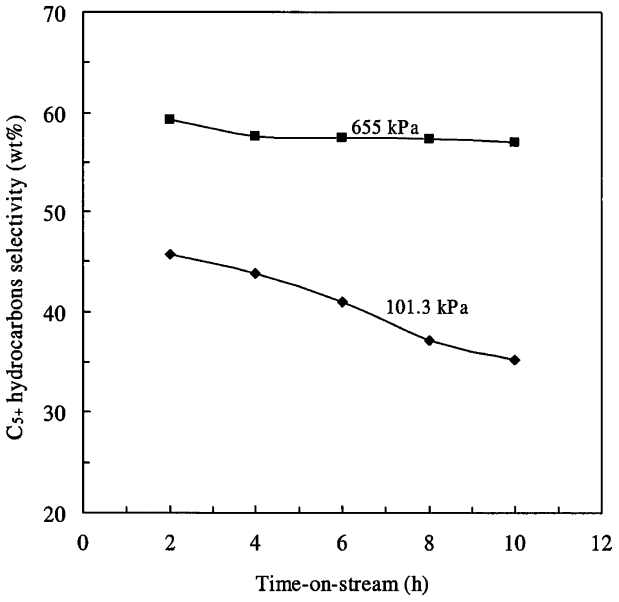

Figure 5. Variation of C_{5+} hydrocarbons selectivity with time-on-stream Conditions:temperature, 533 K; WHSY, 12.3 h^{-1}; catalyst, $Co–Ni/ZrO_2$ (B).

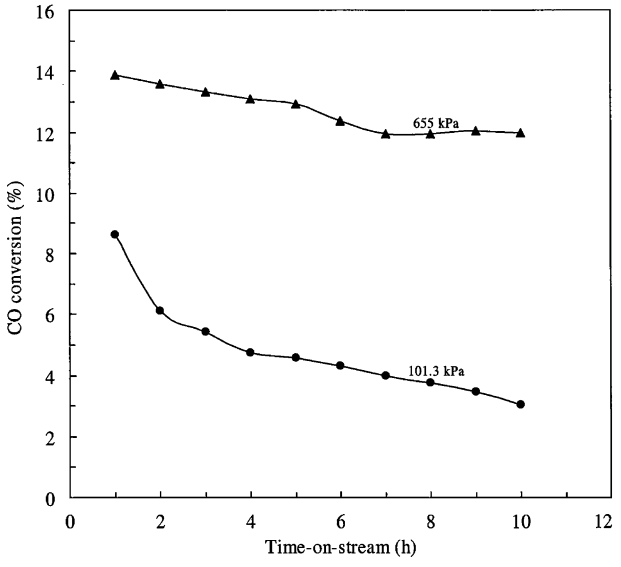

Figure 4. Time-on-stream behavior of Co–Ni/ZrO2 (B) for CO conversion Conditions: temperature, 533 K; WHSY, 12.3 h^{-1}.

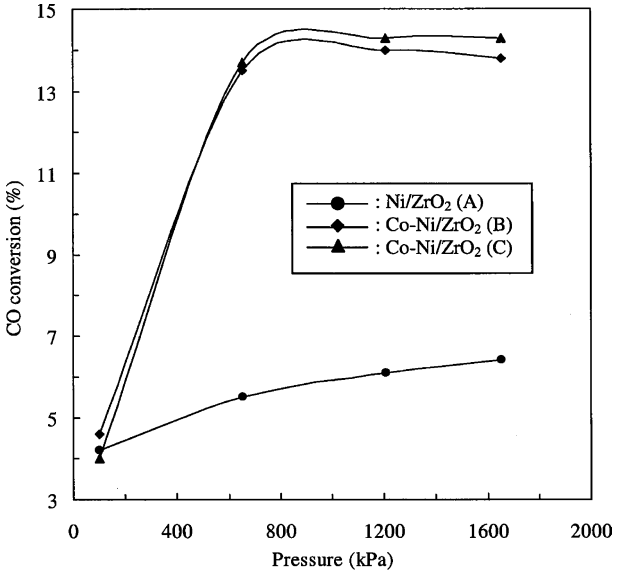

Figure 6. Effect of pressure on conversion of carbon monoxide Conditions:temperature, 533 K; WHSY, 12.3 h^{-1}.

It is widely accepted that the surface CH_x ($x = 1 - 3$) produced over metal catalysts are primary intermediates for the Fischer–Tropsch reactions. These species are formed *via* 15 hydrogenation of surface carbon species, which are produced by dissociation of the adsorbed CO or CO_2 [22]. With increase in pressure, the diffusion of hydrogen molecule from bulk to the surface becomes faster and the conversion of CO increases. After certain pressure (655 kPa), the hydrogenation process becomes surface reaction controlling with no effect of pressure on CO conversion.

With catalyst A, it was observed that the C_1 and C_2 hydrocarbon selectivities increased with increase in pressure, whereas the selectivities for C_3, C_4 and C_{5+} hydrocarbons decrease steadily with increase in pressure. It is well known that in FT synthesis two opposing phenomena, chain propagation and chain termination, control the product distribution. When the chain propagation rate is high, the formation of heavier hydrocarbons is increased. On the other hand, when the chain termination rate predominates, the production of lighter hydrocarbons increases. At high pressure, the hydrogenating property of Ni probably increases further due to higher hydrogen pressure. On account of this, the chain termination rate which is favored at high hydrogen pressure increases thereby lowering the selectivity of C_{5+} hydrocarbons.

Figure 7 shows the effect of pressure on product distribution for catalyst B. As can be seen from this figure, the C_{5+} hydrocarbons selectivity increases with increase in pressure from 101.3 to 655 kPa and then decreases gradually with pressure. The reason for improved C_{5+} hydrocarbons selectivity while operating at high pressure is same as that accounted for improved CO conversion activity at higher pressures. However,

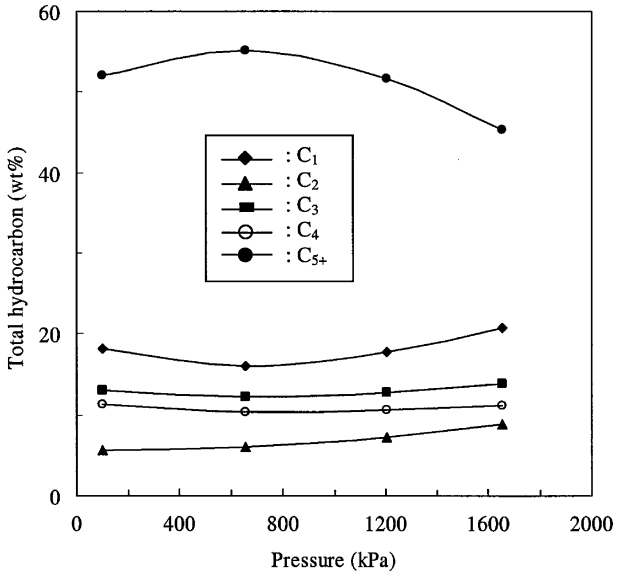

Figure 7. Effect of pressure on product distribution Conditions: temperature, 523 K; WHSY, 9.6 h^{-1}; catalyst, Co–Ni/ZrO_2 (B).

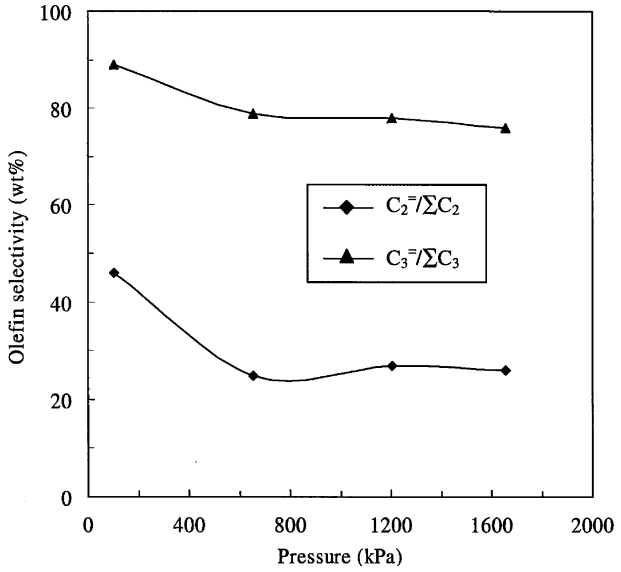

Figure 8. Effect of pressure on olefin selectivity Conditions: temperature, 523 K; WHSY, 9.6 h^{-1}; catalyst, Co–Ni/ZrO_2 (B).

the lowering of heavy hydrocarbon selectivity at pressures greater than 655 kPa may be due to carbonyl formation or wax deposition [27].

The selectivities of $C_2^=$ and $C_3^=$ olefins decrease with increase in pressure up to 655 kPa and then level off as shown in figure 8. As the catalyst becomes more and more hydrogenating in nature at higher pressures, the $C_2^=$ and $C_3^=$ olefins are hydrogenated at higher pressures to corresponding paraffins thereby decreasing their selectivities.

The decrease in selectivities of $C_2^=$ and $C_3^=$ olefins at higher pressures may be explained in another way. At higher pressures, products take longer time to diffuse

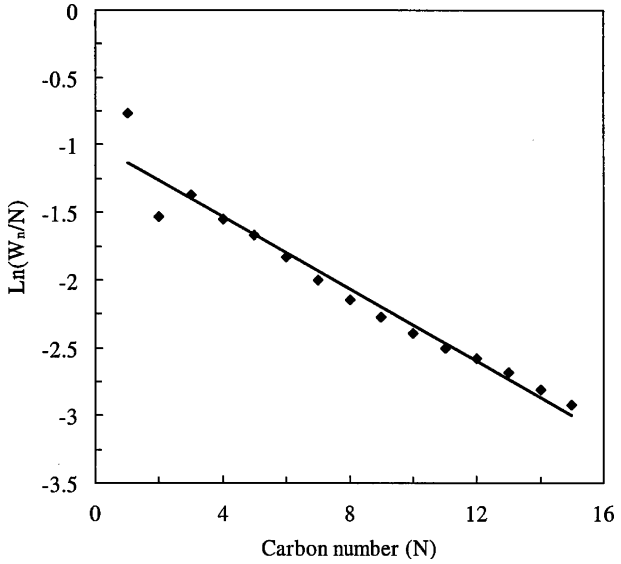

Figure 9. Plot of Anderson–Schultz–Flory polymerization kinetics for Co–Ni/ZrO_2 (B) Conditions:temperature, 533 K; pressure, 655 kPa; WHSY, 12.3 h^{-1}.

Table 3
Comparison of α values of catalysts A, B and C at different pressures

Catalyst	Temperature (K)	Pressure (Kpa)			
		101.3	655	1206	1654
Ni/ZrO2 (A)	523	0.58	0.51	0.43	–
Co–Ni/ZrO2 (B)	533	0.69	0.73	0.73	0.73
Co–Ni/ZrO2 (C)	543	0.70	0.76	0.76	0.76

out of the catalyst pores resulting in more secondary reactions. This results in more hydrogenation of the olefin products resulting in a lower selectivity for olefins.

3.5. *Anderson–Schultz–Flory (ASF) polymerization kinetics*

Products from all the three catalysts were found to obey Anderson–Schultz–Flory (ASF) type polymerization kinetics. A typical ASF plot ($\ln(W_n/N)$ versus N, where N is the carbon number and W_n is the weight fraction of the hydrocarbon with nth carbon number) is shown in figure 9. The α values were calculated from the slope of the straight line. The α values for different catalysts at various pressures are shown in Table 3. It is observed from this table that the value of α for catalyst A decreases with pressure, whereas for catalysts B and C, it increases with increase in pressure from 101.3 to 655 kPa and then levels off at higher pressures. It is interesting to note that the variation of α values is similar to the variation in C_{5+} hydrocarbons selectivity with pressure.

4. Conclusions

The hydrogenation of carbon monoxide was studied over Ni/ZrO_2 and $Co–Ni/ZrO_2$ catalysts. Co–Ni bimetallic catalysts were found to have improved deactivation behavior compared to catalyst containing only Ni. The deactivation behavior of the bimetallic catalyst further improved when operated at higher pressures. A maximum C_{5+} hydrocarbons selectivity of 55 wt% was obtained at 655 kPa pressure, 523 K and 9.6 h^{-1} of WHSV with catalyst containing 4.03 wt% Co and 2.64 wt% Ni. The C_2 and C_3 olefin contents of the products decreased with increase in pressure. Temperature programmed reduction studies of the prepared catalysts showed the presence of metal–support interaction, whereas X-ray diffraction and chemisorption studies with the catalysts indicated highly dispersed nature of the metals within the support matrix.

References

[1] M.E. Dry, Appl. Catal. A. Gen. 189 (1999) 185.
[2] G.L. Ott, T. Fleisch and W.N. Delgass, J. Catal. 60 (1979) 394.
[3] R.L. Verma, L. Dan-Chu, J.F. Mathews and N.N. Bakhshi, Can. J. Chem. Eng. 63 (1985) 72.
[4] D.J. Duvenhage and N.J. Coville, Appl. Catal. A 153 (1997) 43.
[5] E.S. Colley, R.G. Copperthwaite, G.J. Hutchings, G.A. Foulds and N.J. Coville, Appl. Catal. 84 (1992) 1.
[6] H. Chen and A.A. Adesina, Appl. Catal. 112 (1994) 87.
[7] M.E. Cooper and J. Frost, Appl. Catal. 57 (1990) L5.
[8] T. Ishihara, K. Eguchi and H. Arai, Appl. Catal. 30 (1987) 225.
[9] K. Jothirmurugason and S.K. Gangwal, Ind. Eng. Chem. Res. 37 (1998) 1181.
[10] L. Fan, M. Miyauchi and K. Fujimoto, J. Jpn. Pet. Inst. 40 (1997) 298.
[11] H.C. Long, M.L. Turner, P. Fomasiero, J. Kaspar, M. Graziani and P.M. Maitlis, J. Catal. 167 (1997) 172.
[12] C.L. Bianchi and V. Ragaini, J. Catal. 168 (1997) 70.
[13] V. Ragaini, R. Carli, C.L. Bianchi, D. Lorenzetti and G. Vergani, Appl. Catal. A 139 (1996) 17.
[14] V. Ragaini, R. Carli, C.L. Bianchi, D. Lorenzetti, G. Predieri and P. Moggi, Appl. Catal. A 139 (1996) 31.
[15] Y.W. Chen and W.J. Wang, Catal. Today 6 (1989) 105.
[16] L.A. Bruce, M. Hoang, A.E. Hughes and T.W. Tumey, Appl. Catal. A 100 (1993) 51.
[17] A.R. Belambe, R. Oukaci and J. Goodwin, J. Catal. 166 (1997) 8.
[18] T.E. Hoost and J.G. Goodwin, J. Catal. 137 (1992) 22.
[19] E. Kikuchi, M. Matsumoto, T. Takahashi, A. Machino and Y. Morita, Appl. Catal. 10 (1984) 251.
[20] M.A. Vannice and R.L. Garten, J. Catal. 63 (1980) 255.
[21] L.A. Bruce, G.J. Hope and J.F. Mathews, Appl. Catal. 9 (1984) 351.
[22] S. Fujita, N. Hiyoshi and N. Takezawa, Appl. Catal. A 185 (1999) 323.
[23] J.W. Jenkins, B.D. McNicol and S.D. Robertson, Chem. Tech. 7 (1977) 316.
[24] R.L. Varma, J.F. Mathew and N.N. Bakhshi in:Frontiers in Chemical Reaction Engineering, L.K. Doraiswamy, R.A. Mashelkar eds, Vol. II, (1984) 118.
[25] T. Paryjczak, J. Rynkowski and S. Karski, J. Chromatogr. 188 (1980) 254.
[26] C.H. Bartholomew and R.B. Pannell, J. Catal. 65 (1980) 390.
[27] H.H. Stroch, N. Golumbic and R.B. Anderson, The Fischer–Tropsch and Related Synthesis, (John Wiley & Sons, 1952) 323.